GRADIVA

Volume 62 | Issue 11 | November 2023
DOI: 10.5281/zenodo.10350584

Corrosion Resistance Evaluation of NI-AL_2O_3 Coatings on XC18 and E34 Mild Steel

Nora Bouzeghaia [1]*, Mokhtar Benarioua [2] & Mahieddine Naoun [3]

1, 2. Mechanical Structures and Materials Laboratory (MSML), Batna2 University, Algeria.
Email: [1]n.bouzeghaia@univ-batna2.dz (*Corresponding Author), [2]m.benarioua@univ-batna2.dz
3. Corrosion Laboratory, Mechanical Department, Faculty of Technology, Batna2 University, Algeria.
Email: m.naoun@univ-batna2.dz

Abstract

The present study examines nickel's electrodepositing onto XC18 and E34 mild steel surfaces. The Ni/Fe coating has a cathodic behaviour; small cracks or pores cause the underlying material to corrode. Aluminium oxide (Al_2O_3), a complex, dense and stoichiometric composant, was mixed into the nickel matrix to generate a hybrid coating with unique properties. Coatings were produced in a sulfate electrodeposition bath containing different concentrations of Al_2O_3, ranging from 0 to 30 gL^{-1}. To enhance the materials cohesive properties and increase corrosion resistance, a multi-layer electrodeposition technique was employed; a copper layer was initially deposited, followed by the nickel layer deposition. Electrochemical polarisation and weight loss experiments were conducted in a 3.5% NaCl solution to characterize the deposit films. The surfaces morphology and microstructure were analyzed using X-ray diffraction and scanning electron microscopy (SEM). The results indicate a significant decrease in corrosion rates, with minimal rates seen at Al_2O_3 concentrations ranging between 25 to 30 gL^{-1} for XC18 and 25 gL^{-1} for E34. The corrosion resistance of the composite Ni-AL_2O_3 deposit might be attributed to the successful occlusion of Al_2O_3 particles into the nickel pores. In the case of E34 specimens, the corrosion rates exhibited an escalation once the concentration of Al_2O_3 surpassed 25 gL^{-1}.

Keywords: Ni-Al_2O_3, Sulfated Nickel Bath, Corrosion, Electrodeposition, Coating Pores.

1. INTRODUCTION

Particle-reinforced metal matrix composites are widely used in various technical applications due to their higher characteristics, such as increased hardness, improved durability, and improved corrosion resistance [1-3]. Aluminium Oxide (Al_2O_3) is distinguished for its remarkable hardness, high melting point, and great chemical stability [4]. The use of nickel coatings has been employed to enhance the surface properties of several metals. This approach has multiple advantages, such as; improved resistance to corrosion and greater protection against wear. However, ordinary nickel coatings are not resistant due to their basic limits.

The addition of Al_2O_3 particles to Ni coatings has been shown to significantly improve their corrosion resistance, as indicated by research conducted by Aruna et al. [5], Feng et al. [6], and Lu et al. [7]. The improvement shown in this study is associated with the optimisation of Ni crystalline structure and modifications in the preference orientation of the composite coatings, as reported by Feng et al. Moreover, the coatings characteristics are influenced by the particular type of alumina particles employed. Aruna et al. have observed that the use of pure gamma-alumina enhances corrosion resistance, whilst pure alpha-alumina enhances wear resistance. The corrosion resistance of the composite coating is significantly influenced by the

Volume 62 | Issue 11 | November 2023
DOI: 10.5281/zenodo.10350584

quantity of Al_2O_3 included into the Ni matrix. According to the research conducted by Lu et al., it was found that the optimal corrosion resistance was reached by incorporating 8 gL^{-1} of Al_2O_3 particles into the plating solution [5]. The work conducted by Feng et al. also showed an important corrosion resistance rise when including nano-Al_2O_3 particles into the Ni matrix. Specifically, the Ni–7.58 wt.% Al_2O_3 composite coating demonstrated superior performance in this regard [4].

Chen et al. highlighted the importance of surfactants for a more even distribution of Al_2O_3 particles within the nickel matrix, which contributes to improved wear resistance in the coatings [8]. Additionally, Gadhari's et al. work underlined the critical impact of alumina particle concentration and annealing temperature on the corrosion resistance of these composites [9]. Collectively, these studies underscore the necessity of optimizing Al_2O_3 concentration and other process parameters to maximize the corrosion resistance of Ni-Al_2O_3 composite coatings. The current study aims to conduct an analysis on determining the ideal concentration of nanoparticles to be incorporated into nickel coating, within a sulfate bath. The objective is to achieve optimal protection against the corrosion process of steel coated with this nickel layer, particularly in a salt solution with a concentration of 35 gL^{-1}.

2. EXPERIMENTAL

Materials: Two types of mild steel were used for the development of the deposits; XC18 and E34 substrats, Table 1.

Table 1: Samples chemical composition

Eléments	XC 18 [%]	E 34 [%]
C	0.220	0.0600
S	0.032	0.0200
Si	0.220	0.0300
Mn	0.760	0.3600
P	0.020	0.0030
Al	0.008	0.0080
Cu	0.215	0.0640
Ni	0.117	0.0200
Cr	0.048	0.0240
V	0.002	0.0080
Ti	0.003	0.0030
Nb	0.002	0.0050
Mo	0.022	0.0080
Sn	0.011	0.0083

2.1. Realization of specimens

XC18 Steel Bars: Machined into flat rectangular species measuring 100 x 12 x 3 mm thickness.

Wire Meshes: Cylindrical wire meshes with 6 mm diameter were cut into 60 mm length pieces.

2.2 Specimens surface preparation

2.2.1. Surface finish (Polishing)

Flat test pieces after machining were polished with SiC paper 180, 400, 600, and 1000.

Cylindrical specimens were ground down to 4 mm diameter and polished.

Volume 62 | Issue 11 | November 2023
DOI: 10.5281/zenodo.10350584

2.2.2. Specimens surface cleaning (Degreasing)

The test specimens were degreased ultrasonically in an ethanol solution for 5 minutes, then rinsed in distilled water and dried in hot air.

2.3. Electroplating

2.3.1 Electroplating Baths composition

Pre-Copper plating: Before the nickel deposit, a pre-copper plating was carried out on all the test pieces. The composition of the bath is detailed in Table 2.

Nickel deposits: They were obtained from a sulphated nickel bath. The composition of the nickel-plating bath is provided in Table 3.

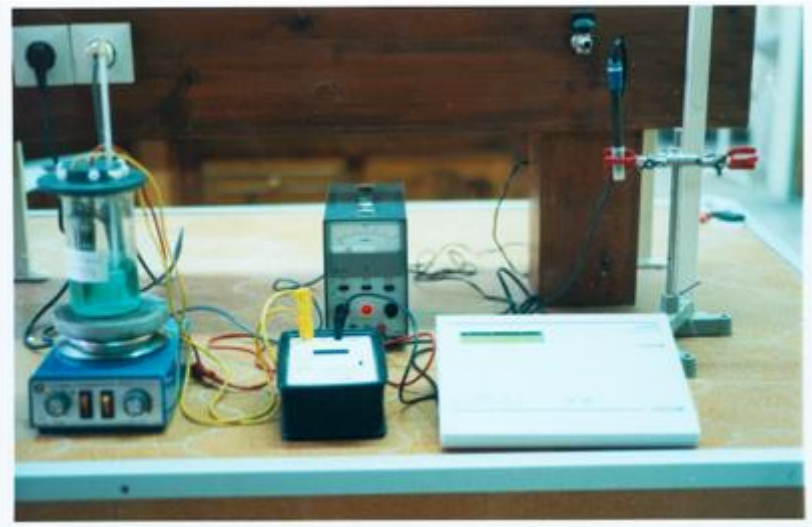

Fig 1: Experimental Setup

Table 2: Copper bath composition [10]

Constituent	Content
Copper acetate $Cu(C_2H_3O_2)_2$	18 à 20 gL^{-1}
Potassium cyanide KCN	20 à 22 gL^{-1}
Potassium carbonate K_2CO_3	30 à 40 gL^{-1}
Ammonia NH_3	15 à 20 mlL^{-1}
Sodium Bisulfite $NaHSO_4$	15 à 20 mlL^{-1}

Table 3: Composition of the sulfated nickel bath [11]

Constituent	Content [gL^{-1}]
Nickel(II) sulfate hexahydrate $NiSO_4+6H_2O$	13.1425
Ammonium sulfate $(NH_4)_2SO_4$	39.642
Sodium sulfate decahydrate $Na_2SO_4+10H_2O$	14.204
Boric acid H_3BO_3	6.183

Volume 62 | Issue 11 | November 2023
DOI: 10.5281/zenodo.10350584

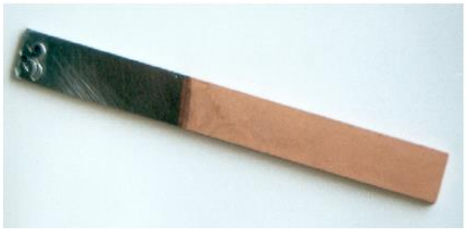

Fig 2: Copper deposit on XC18 flat specimen.

Fig 3: Copper deposit on E34 cylindrical specimen.

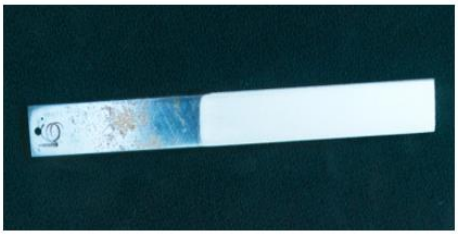

Fig 4: Nickel deposit on XC18 flat specimen.

Fig 5: Nickel deposit on E34 cylindrical specimen.

2.3 Composite coating characterization

2.3.1 Mass loss test

The electrolyte used is a 3.5% sodium chloride solution, adjusted to a pH near 8 with a buffer mixture. Test specimens were initially weighed and then coated with an insulating winding varnish. They were left exposed to air for two days to ensure thorough drying of the varnish. For the corrosion test, the specimens were suspended in a beaker of electrolyte solution—300 ml for flat specimens and 200 ml for cylindrical ones—for six days. Post-immersion, the specimens were cleaned with a nylon brush to remove corrosion byproducts and then in acetone for varnish removal, using ultrasonic cleaning. Finally, they were rinsed with distilled water, dried, and weighed again to evaluate the impact of the corrosion test.

2.3.2 Electrochemical polarization

Polarization tests were conducted in an electrolyte of distilled water containing 3.5% NaCl, using a Voltalab PGP 201 Potentiostat and a three-electrode cell; the working electrode, a platinum counter electrode, and a saturated calomel reference electrode. The sweep was carried out at a rate of 20 mV/min.

2.3.3 X-Ray Diffraction Analysis (XRD)

The X-ray diffraction spectra were recorded using a PANalytical X'PERT PRO MRD diffractometer, equipped with a copper anode X-ray tube. An acquisition time of 5 seconds per angular step of 0.04° was used over the range between 20° and 100° (2θ).

2.3.4 Scanning Electron Microscopy

The coatings surface morphology was examined using a HITACHI FE-SEM S4800 Scanning Electron Microscope.

Volume 62 | Issue 11 | November 2023
DOI: 10.5281/zenodo.10350584

3. RESULTS AND DISCUSSION

3.1 Corrosion results

3.1.1 Mass loss results

- Corrosion Rate calculation

A difference in mass between the first weighing (before test) and the second weighing (after test) results in a corrosion rate given by the following formula:

$$Taux_{corr.} = \frac{\Delta m \cdot 10}{\rho \cdot S_{immg}} \times \frac{365}{t} \quad \text{[mm/an]} \qquad (1)$$

Where:

$\Delta m = m_1 - m_2$ [g] mass difference; (2)

m_1 [g] mass before immersion;

m_2 [g] mass after immersion;

ρ [g/cm^3] steel density;

t [days] time of immersion ;

S_{immg} [cm^2] submerged surface area.

The calculated values are reported in tables 4, 5, 6 and 7.

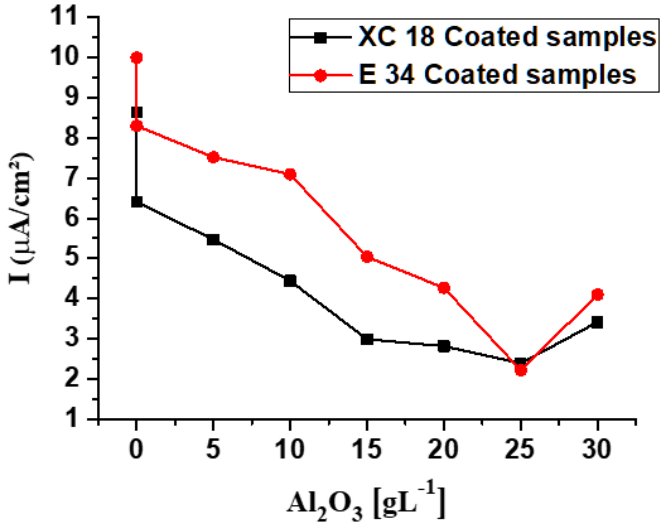

Fig 6: Mass loss corrosion rate of XC18 and E34 specimens coated in a sulfated nickel bath.

Table 4: Mass loss corrosion rate of the XC18 uncoated specimen

Mass Before test [g]	Mass After test [g]	Mass Difference [g]	Immerged Surface [cm²]	Corrosion Rate [mm/an]	Curent Density [µ A/cm²]
14.3548	14.3383	0.0165	12,7014	0.101	8.6311

Volume 62 | Issue 11 | November 2023
DOI: 10.5281/zenodo.10350584

Table 5: Mass loss Corrosion rate of XC18 specimens coated in a Nickel sulfate bath

Al_2O_3 [gL^{-1}]	Mass Before test [g]	Masse After test [g]	Mass Difference [g]	Immerged Surface [cm^2]	Corrosion rate [mm/an]	Curent Density [µ A/cm^2]
0	14,1577	14,1456	0,0121	12,5664	0.075	6.4092
05	14,7463	14,7359	0,0104	12,7066	0.064	5.4692
10	14,8853	14,8720	0,0133	12,7066	0.052	4.4437
15	14,5606	14,5550	0,0056	12,3406	0.035	2.9910
20	14,7850	14,7717	0,0133	12,5846	0.040	2.8210
25	14,7340	14,7295	0,0045	12,7567	0.028	2.3928
30	14,3973	14,3910	0,0063	12,5715	0.040	3.4182

Table 6: Mass loss corrosion rate of the E34 uncoated specimen

Mass Before test [g]	Masse After test [g]	Mass Difference [g]	Immerged Surface cm^2]	Corrosion Rate [mm/an]	Curent Density [µ A/cm^2]
5,7726	5.7607	0,0119	5,4648	0.117	9.9984

Table 7: Mass loss Corrosion rate of E34 specimens coated in a Nickel sulfate bath

Al_2O_3 [gL^{-1}]	Mass Before test [g]	Masse After test [g]	Mass Difference [g]	Immerged Surface [cm^2]	Corrosion rate [mm/an]	Curent Density [µ A/cm^2]
05	6,0300	6,0248	0,0052	4,6072	0,088	7.5202
10	5,2402	5.2357	0,0045	4,2003	0,083	7.0929
15	6,0000	5,9961	0,0039	5,1071	0,059	5.0419
20	5,6791	5,6763	0,0028	4,3103	0,050	4.2728
25	5,8823	5.8809	0,0014	4,3433	0,026	2.2219
30	5,8652	5.8625	0,0027	4,3652	0,048	4.1019

Fig. 6 shows that for both XC18 and E34 specimens, the addition of Al_2O_3 to the nickel sulfate bath appears to reduce the corrosion rate significantly compared to the uncoated specimens. This suggests that Al_2O_3 enhances the corrosion resistance of the nickel coating.

The corrosion rate generally decreases as the concentration of Al_2O_3 increases, indicating that higher concentrations of Al_2O_3 are more effective in improving corrosion resistance. The lowest corrosion rates for both XC18 and E34 specimens are observed at 25 gL^{-1} Al_2O_3 concentration, suggesting an optimal concentration for corrosion resistance enhancement.

This trend aligns with the notion that the inclusion of Al_2O_3 particles in the nickel matrix can improve the coating's density and reduce its porosity, thus enhancing its protective capabilities against corrosion [12-15].

Volume 62 | Issue 11 | November 2023
DOI: 10.5281/zenodo.10350584

3.2. Electrochemical polarization results

The corrosion rates estimated by this technique are given in Figure 7 and Table 8.

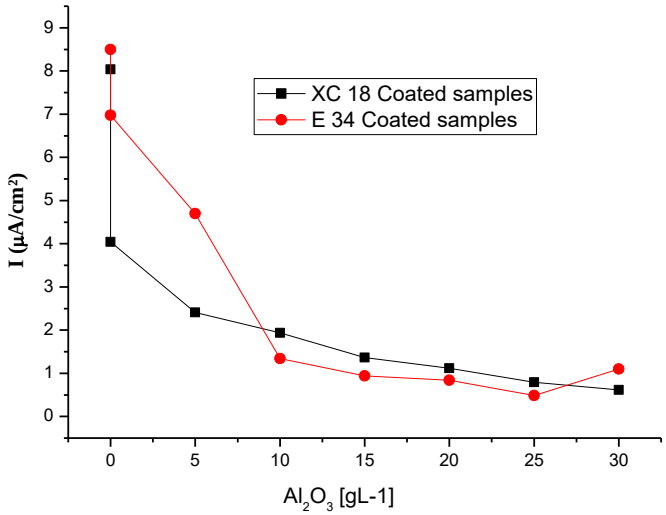

Fig 7: Electrochemical polarization corrosion rate of XC 18 and E 34 specimens coated in a sulfated nickel bath.

Table 8: Electrochemical polarization corrosion rate of XC18 and E34 specimens coated in a Nickel sulfate bath.

Al_2O_3 [gL^{-1}]	XC18 Specimens		E34 Specimens	
	Corrosion rate [mm/an]	Curent Density [μ A/cm²]	Corrosion rate [mm/an]	Curent Density [µ A/cm²]
0	0.094	8.0366	0.099	8.5
0	0.047	4.0435	0.082	6.9763
5	0.036	2.4062	0.055	4.7000
10	0.023	1.9379	0.016	1.3429
15	0.015	1.3640	0.011	0.9378
20	0.013	1.1155	0.010	0.8404
25	0.009	0.7937	0.005	0.4844
30	0.008	0.6140	0.012	1.0975

According to Figure 4, we observe a gradual decrease in the corrosion rate until a minimum value is reached. This value corresponds to an Al_2O_3 concentration located in the range of [25, 30] $gL^{-1}$for the examined steel XC 18, and at a concentration of 25 gL^{-1} in the case of E 34 steel. Moreover, for the E 34 steel, an increase in the corrosion rate is observed beyond the concentration of 25 gL^{-1} of Al_2O_3. The variations in the corrosion rate have the same appearance as those obtained by the lost mass technique.

This suggests that the decrease is linked to the addition of Al_2O_3 in the electrodeposition baths, which are deposited in the pores of the coating, thus leading to the reduction of pitting attacks by aggressive chlorine anions

Volume 62 | Issue 11 | November 2023
DOI: 10.5281/zenodo.10350584

3.3. X-Ray Analysis

The results of the X-ray diffraction (XRD) analysis of the composites (Ni-Al_2O_3) with 10 gL^{-1} of Al_2O_3 concentration is shown in the Figure 8. The observed peaks at (111), (200), (220), and (222) indicate the presence of pure nickel, confirming its face-centered cubic (FCC) crystal structure [16]. In addition to the nickel peaks, a distinct peak at (134) was identified, corresponding to the α–Al_2O_3 phase [17], suggesting the successful incorporation of Al_2O_3 into the composite. The absence of other significant peaks suggests a high purity of the composite materials and a relatively clean electrodeposition process.

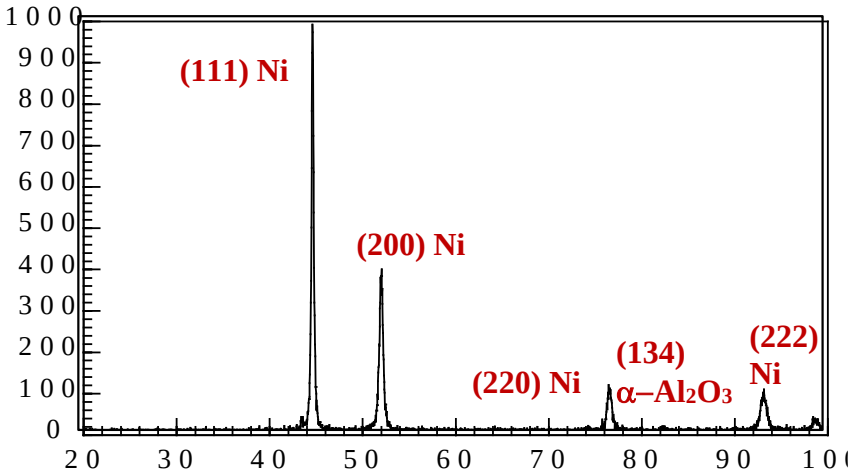

Fig 8: XRD analysis of a sample coated in a sulfate bath in the presence of 10 gL^{-1} of Al_2O_3

4. SEM RESULTS

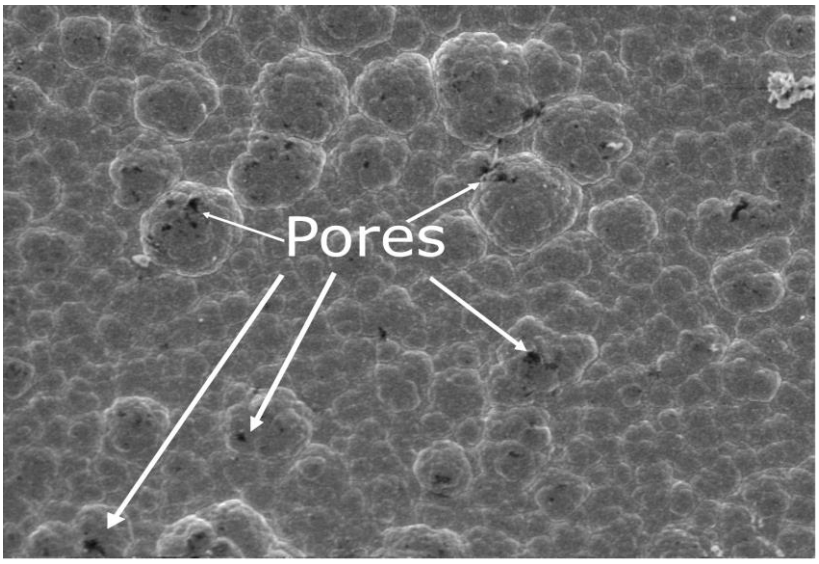

Fig 9: Nickel sulfate coating without the addition of Al_2O_3 (x 740)

Volume 62 | Issue 11 | November 2023
DOI: 10.5281/zenodo.10350584

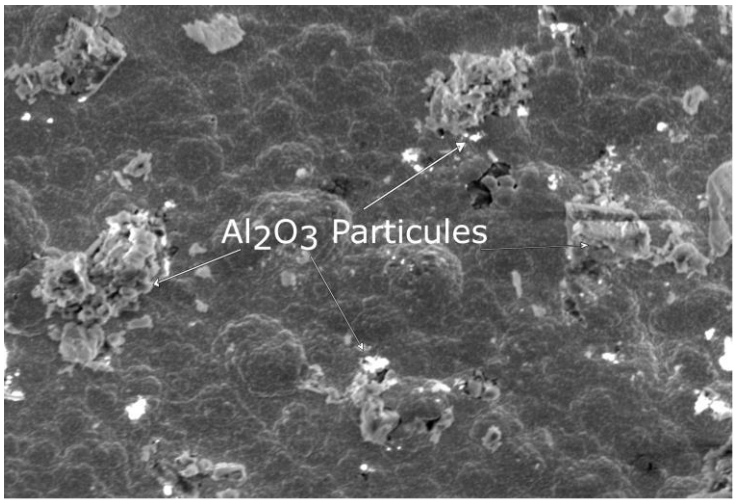

Fig 10: Nickel sulfate coating in the presence of 25 gL^{-1} of Al_2O_3 (x 740)

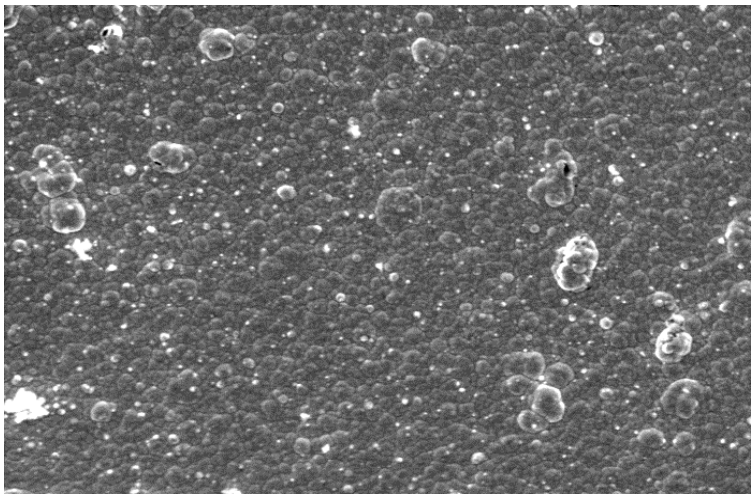

Fig 11: Nickel sulfate coating in the presence of 25 gL^{-1} of Al_2O_3 (x 370)

Fig. 9 shows a nickel sulfate coating devoid of any Al_2O_3 additives. The absence of Al_2O_3 reinforcing particles results in a smoother but potentially more porous structure, as compared to composites. The higher porosity leads to increased corrosion rates since more surface area of the underlying substrate is exposed to corrosive environments

Fig. 10 depicts the nickel sulfate coating integrated with 25 gL^{-1} of Al_2O_3. The addition of Al_2O_3 is expected to result in a more heterogeneous microstructure. The Al_2O_3 particles act as barriers within the Ni matrix, potentially reducing porosity by obstructing the formation of large voids during the plating process. This effect is visible here as a more irregular surface texture compared to the unmodified Ni coating.

Fig. 11 Taken at a lower magnification, this image offers a broader view of the Ni- Al_2O_3 composite coating. The distribution and impact of Al_2O_3 particles on the coating's overall microstructure can be observed. A more uniform dispersion of these particles can lead to a significant reduction in porosity across the coating enhancing the corrosion resistance of the composite.

Volume 62 | Issue 11 | November 2023
DOI: 10.5281/zenodo.10350584

5. CONCLUSION

The study investigates the impact of incorporating Al_2O_3 nanoparticles into nickel coatings electrodeposited on XC 18 and E34 mild steel substrates. Key findings include:

- A significant decrease in corrosion rates with increasing Al_2O_3 concentrations, with the lowest rates observed at 25-30 gL^{-1} for XC 18 and 25 gL^{-1} for E34.
- For E34, corrosion rates increased when Al_2O_3 concentration exceeded 25 gL^{-1}.
- The presence of Al_2O_3 particles effectively seals coating pores, reducing corrosion susceptibility.
- Optimal Al_2O_3 concentration for enhanced corrosion resistance is around 25 gL^{-1}.
- The study corroborates findings using both mass loss and electrochemical polarization methods, confirming the effectiveness of Al_2O_3 in improving corrosion resistance of Ni coatings.

References

1) Saravanan, C. et al. “Effect of Particulate Reinforced Aluminium Metal Matrix Composite -A Review.” *Mechanics and Mechanical Engineering* 19 (2015): n. pag.

2) Bihari, Bagesh and Ashutosh Kumar Singh. “An Overview on Different Processing Parameters in Particulate Reinforced Metal Matrix Composite Fabricated by Stir Casting Process.” *International Journal of Engineering Research and Applications* 7 (2017): 42-48.

3) Casati, Riccardo and Maurizio Vedani. “Metal Matrix Composites Reinforced by Nano-Particles—A Review.” (2014).

4) Richards, Gavin. “Aluminum Oxide Ceramics.” *Advanced Ceramic Materials* (1991): 16-20.

5) Aruna, S. T. et al. “Corrosion- and wear-resistant properties of Ni–Al_2O_3 composite coatings containing various forms of alumina.” *Journal of Applied Electrochemistry* 41 (2011): 461-468.

6) Feng, Qiuyuan et al. “Investigation on the corrosion and oxidation resistance of Ni–Al2O3 nano-composite coatings prepared by sediment co-deposition.” *Surface & Coatings Technology* 202 (2008): 4137-4144.

7) Lu, Jianxiang et al. “Effects of Content of Al_2O_3 Particles and Heat Treatment on Corrosion Resistance of Ni-P-Al_2O_3 Composite Coatings.” *Advanced Materials Research* 105-106 (2010): 441 - 443.

8) Chen, Li et al. “Effect of surfactant on the electrodeposition and wear resistance of Ni–Al2O3 composite coatings.” *Materials Science and Engineering A-structural Materials Properties Microstructure and Processing* 434 (2006): 319-325.

9) Gadhari, Prasanna and Prasanta Kumar Sahoo. “Improvement of Corrosion Resistance of Ni-P-Al2O3 Composite Coating by Optimizing Process Parameters Using Potentiodynamic Polarization Test.” *Portugaliae Electrochimica Acta* 32 (2014): 137-156.

Volume 62 | Issue 11 | November 2023
DOI: 10.5281/zenodo.10350584

10) Y. Badé, Revêtements Métalliques par Voie Electrolytique, Cuivrage M1605, Technique de l'Ingénieur, (1990).

11) Y. Badé, Revêtements Métalliques par Voie Electrolytique, Nickelage, M 1610, Technique de l'Ingénieur, 2000.

12) S. Karthikeyan, B. Ramamoorthy, Effect of reducing agent and nano Al2O3 particles on the properties of electroless Ni–P coating, Applied Surface Science, Volume 307, 2014, Pages 654-660, ISSN 0169-4332, https://doi.org/10.1016/j.apsusc.2014.04.092.

13) iuyuan Feng, Tingju Li, Hongyun Yue, Kai Qi, Fudong Bai, Junze Jin, Preparation and characterization of nickel nano-Al2O3 composite coatings by sediment co-deposition, Applied Surface Science, Volume 254, Issue 8, 2008, Pages 2262-2268, ISSN 0169-4332,
https://doi.org/10.1016/j.apsusc.2007.09.014.

14) H. Gül, F. Kılıç, S. Aslan, A. Alp, H. Akbulut, Characteristics of electro-co-deposited Ni–Al2O3 nano-particle reinforced metal matrix composite (MMC) coatings, Wear, Volume 267, Issues 5–8, 2009, Pages 976-990, ISSN 0043-1648, https://doi.org/10.1016/j.wear.2008.12.022.

15) R.A. Shakoor, Ramazan Kahraman, Umesh Waware, Yuxin Wang, Wei Gao, Properties of electrodeposited Ni–B–Al2O3 composite coatings, Materials & Design, Volume 64, 2014, Pages 127-135, ISSN 0261-3069, https://doi.org/10.1016/j.matdes.2014.07.026.

16) Masoudi, Mehran et al. "Characterization of novel Ni–Al2O3–SiC nanocomposite coatings synthesized by co-electrodeposition." *Applied Nanoscience* 4 (2014): 649-656.

17) Mohammed, Adnan A. et al. "Preparation and investigation of the structural properties of α-Al_2O_3 nanoparticles using the sol-gel method." *Chemical Data Collections* 29 (2020): 100531. Mohammed, Adnan A. et al. "Preparation and investigation of the structural properties of α-Al2O3 nanoparticles using the sol-gel method." *Chemical Data Collections* 29 (2020): 100531.